Int. J. Electrochem. Sci., 15 **(2020)** 7359 – 7369, doi: 10.20964/2020.08.31

International Journal of
ELECTROCHEMICAL
SCIENCE
www.electrochemsci.org

Electrocatalytic Determination of Isoprenaline Using well-shaped Cerium Oxide Nanorods Modified Glassy Carbon Electrode

Natesan Manjula[1], *Subbarayan Sumithra*[1],*Tse-Wei Chen*[2], *Shen-Ming Chen*[*1]

[1] Department of Chemical Engineering and Biotechnology, National Taipei University of Technology, Taipei 106, Taiwan, ROC
[2] Department of Materials, Imperial College London, London, SW7 2AZ, United Kingdom
[*]E-mail: smchen78@ms15.hinet.net

Received: 2 April 2020 / *Accepted:* 28 May 2020 / *Published:* 10 July 2020

We describe the electrochemical detection of isoprenaline (ISPN) using a well-shaped cerium oxide nanorods (CeO_2 NRs) modified with a glassy carbon electrode. The characterization of as-synthesized CeO_2 NRs by X-ray diffraction (XRD), Field emission scanning electron microscopy (FE-SEM), Fourier transform infrared (FT-IR). Differential pulse voltammetry (DPV), electrochemical impedance spectroscopy (EIS), and cyclic voltammetry (CV) were used to evaluate the electrochemical performance of the as-proposed sensor. The CeO_2 NRs/GCE exhibits an excellent electro-oxidation performance towards the ISPN at the lower oxidation potential of 0.20 V. Under the optimal conditions, the good linearity was obtained for ISPN concentration range from 0.04 to 539 μM with a low detection limit (LOD) is 18 nM. Also, the constructed sensor has good anti-interference ability, stability, and reproducibility. Finally, the practical applicability of the fabricated electrode assessed by the detection of ISPN in human urine samples with acceptable recovery.

Keywords: Cerium oxide, nanorods, isoprenaline, sensors, voltammetry

1. INTRODUCTION

The human body contains adrenergic receptors, and their roles are damaged by several significant biochemical and physiological processes [1]. Isoprenaline (ISPN) is chemically known as 4-[1-hydroxy-2-[(1-methyl-ethyl)-amino]ethyl]-1,2-benzenediol [2]. It is a sympathomimetic beta-adrenergic agonist medication and one of the important catecholamine drugs [3,4]. Food and Drug Administration was approved the ISPN is trace-amine associated receptor 1 (TAAR 1) and potent non-selective beta-adrenergic agonist [5]. It is extremely utilized in the treatment of (slow heart attack) bradycardia [6], allergic emergencies, bronchial asthma [7], glaucoma, and as a styptic [2]. Nonetheless, the excess of

ISPN can cause arrhythmia and heart attack [3]. Therefore, many side effects create the use of ISPN, which may include anxiety, flushing, shaking, chest pain, and headache [8]. So, it is necessary to develop a simple and more effective method for ISPN detection in pharmaceutical preparations and clinical tests [9]. To date, numerous methods have been used for determining the ISPN including fluorescence [8], spectrofluorimetric [10], chromatography [7], chemiluminescence, nuclear magnetic resonance spectroscopy [11]. However, the abovementioned methods had been affected by the drawbacks of time-consuming, costly equipment [10], low sensitivity, and problematic procedures [8]. Compared with those methods the electrochemical method is simple, fast, low cost [12], high sensitivity, and selectivity [11].

Cerium oxide is unique and most significant functional rare earth metal. In current centuries, various studies have been exposed to ceria and their catalytic properties including hydrogen electro-oxidation and photocatalytic oxidation [12,13]. The application and properties of cerium oxide consist of catalyst, luminescent sensor, energy, and magnetic data storage [12,14], polishing materials, absorbing pollutants [15], oxygen ion conductivity, and high mechanical strength, etc [13]. Cerium oxide has been used for numerous electrochemical applications because of their electrical conductivity, nontoxicity, large surface area, biocompatibility, and their excellent electrochemical features [16]. For illustration, G. Manibalan *et al*. performed the electrochemical detection of L-cysteine biomolecule using CeO_2-based heterostructure nanocomposite [17]. A. Sangili *et al*. developed an electrochemical detection of nitrobenzene in water samples using ultra-small cerium oxide nanoparticles [16].

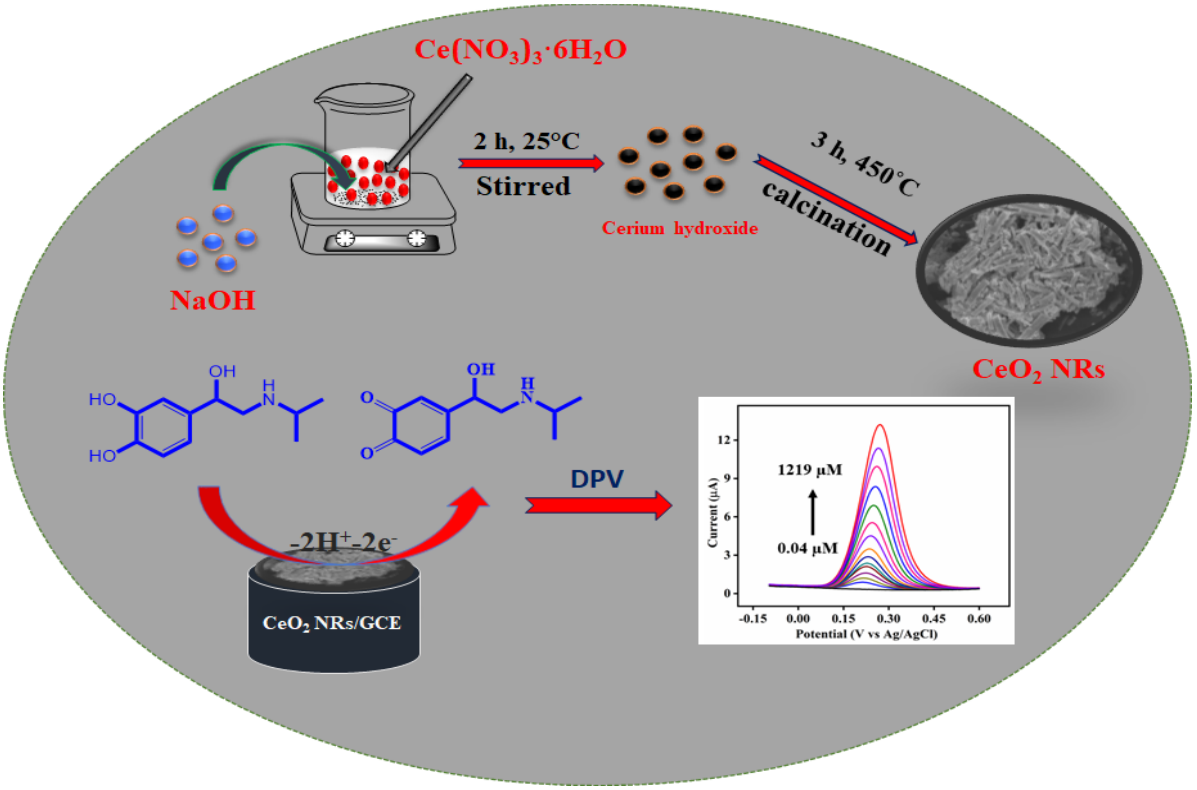

Scheme 1. Schematic representation of CeO_2 NRs preparation and ISPN sensing

In the present study, cerium oxide nanorods were prepared by a simple one-step coprecipitation method assisted by sodium hydroxide. The electrochemical properties of the CeO_2 NRs fabricated electrode and its electro-oxidation response towards ISPN were studied through the cyclic voltammetry (CV). Under the optimized conditions, the proposed electrode exhibits high selectivity, wide linear range, low oxidation potential, and good stability. To the best of our knowledge, there has been no literature on the CeO_2 NRs/GCE as an electrochemical sensor for ISPN detection. Finally, the fabricated electrode was used towards ISPN determination in human urine samples with acceptable recovery.

2. EXPERIMENTS

2.1 Chemicals and Apparatus

Cerium nitrate hexahydrate, sodium hydroxide, isoprenaline, sodium dihydrogen phosphate, and disodium hydrogen phosphate were procured from (www.sigma-aldrich.com) Sigma-Aldrich. And potassium ferricyanide, potassium ferrocyanide, potassium chloride all are GR grade, were brought from Merck. All the chemicals are used in this study were of analytical grade and without further refinement. The phosphate buffer (PBS) pH 7.0, 0.05 M is employed as the supporting electrolyte and it is prepared by dissolving a requisite amount of Na_2HPO_4 and NaH_2PO_4 in DI water. Workstation CHI 1205B and CHI 900 with a conventional three-electrode arrangement were used for all the electrochemical experiments. The CeO_2 NRs modified glassy carbon electrode as a working electrode, saturated Ag/AgCl and platinum wire (1 mm diameter) as a reference electrode and counter electrode respectively. All the electrochemical characterizations were performed in an inert (N_2) atmosphere. XRD pattern was analyzed on (XPERT-PRO, k=1.54A) and using Cu kα radiation. FTIR spectrum was recorded by JASCO FT/IR-6600 spectrophotometer. Field Emission Scanning Electron Microscopy (Hitachi S-3000H) was used to investigate the surface morphology of as-prepared nanomaterial.

2.2 Synthesis of cerium oxide nanorods

Cerium oxide nanorods were prepared in the presence of sodium hydroxide by a simple co-precipitation method. Thereby, the required amount of cerium nitrate hexahydrate is dissolved in 50 mL of pure DI water and allowed to ultra-sonicated about 15 min to obtain the clear dispersion. Then, the solution was stirred vigorously under ambient temperature. After sodium hydroxide (0.5 M, NaOH) was gradually added into the above solution and suddenly the color change is colorless to turbidity. The mixture was allowed to stir for 3 h at ambient temperature, then the obtained suspension is washed more than three times with DI water and ethanol to remove the unreacted particles and dried in an oven. Consecutively, the dried product was calcinated for 3 h at 450˚C to attain the final product of CeO_2 NRs.

2.3 Fabrication of GCE modified with CeO_2 NRs

Before the surface modification, the bare GC electrode was polished with 1.0 and 0.5 μm alumina powder. After that, the electrode was carefully washed with DI water for 10 min by ultrasonically. 2

mg/ml of CeO_2 NRs dispersed in 1 mL of deionized water and sonicated for 20 min. Finally, CeO_2 NRs fabricated GCE was done by 6 µL of CeO_2 NRs suspension was drop cast on the surface of well-cleaned GCE and dried in an oven. This procedure was followed for all the below electrochemical studies.

3. RESULT AND DISCUSSION

3.1 Characterization

3.1.1 XRD, FT-IR, and FE-SEM analysis

The crystalline nature of as-prepared CeO_2 nanorods was examined by X-ray diffraction and the obtained XRD results are shown in Figure 1A. The CeO_2 exhibits the significant diffraction peaks at 28.54°, 33.07°, 47.47°, 56.33°, 59.07°, 69.40°, 76.68°, and 79.06° can be indexed as the (111), (200),(200), (311), (222), (400), (331), and (420) diffraction planes of cubic phase with respective JCPDS-PDF Card No. 01-081-0792 [18][13]. This result indicates there are no other peaks that were observed for desirable impurities such as $Ce(OH)_2$ in as-synthesized CeO_2. Finally, the observed major peaks from Figure 1A strongly confirms the formation of cerium oxide. The infrared spectra (FT-IR) of as-prepared cerium oxide nanorods were recorded in the range of wavenumber (400 – 4000 cm^{-1}), using the KBr pellet method, is shown in Figure 2A. The strong and broadband located at approximately 3418 cm^{-1} is ascribed to hydrogen-bonded OH-stretching vibration mode, 1629 cm^{-1} is bending vibration mode of (O–H) hydroxyl group [19] absorption band positioned at 1378 cm^{-1} is (N-O) stretching, the peak appeared at 1545 cm^{-1} is (C=C) functional group [20]. The large peak at 476 cm^{-1} is due to the stretching vibration of O-Ce-O [21]. XRD and FT-IR spectrum results confirmed the formation of pure cerium oxide.

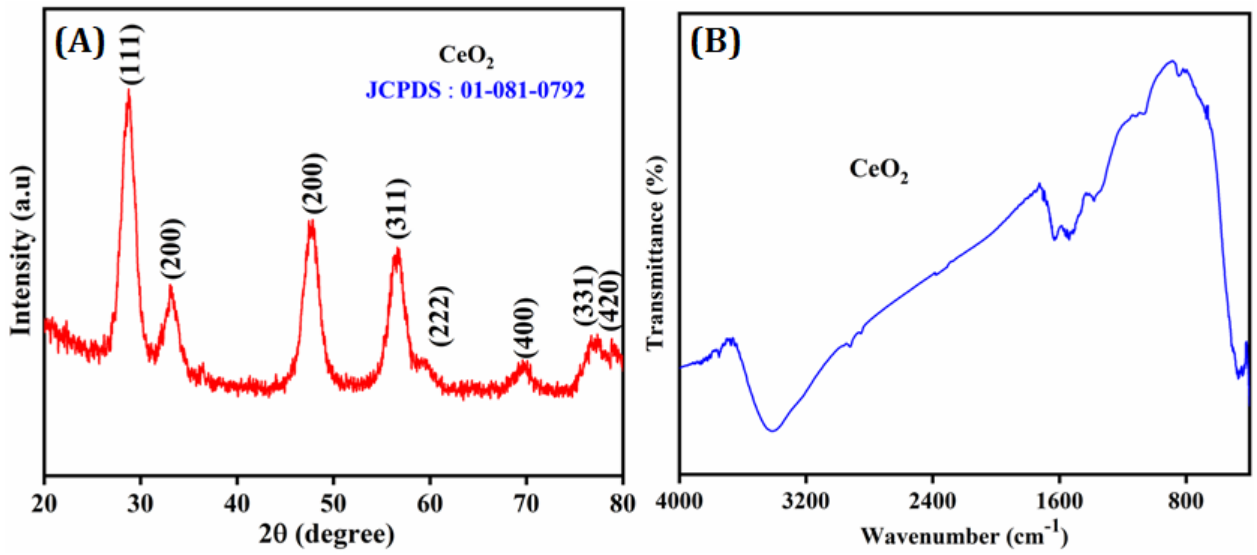

Figure 1. (A) X-ray diffraction spectrum of CeO_2 NRs, **(B)** FT-IR spectrum of CeO_2 NRs

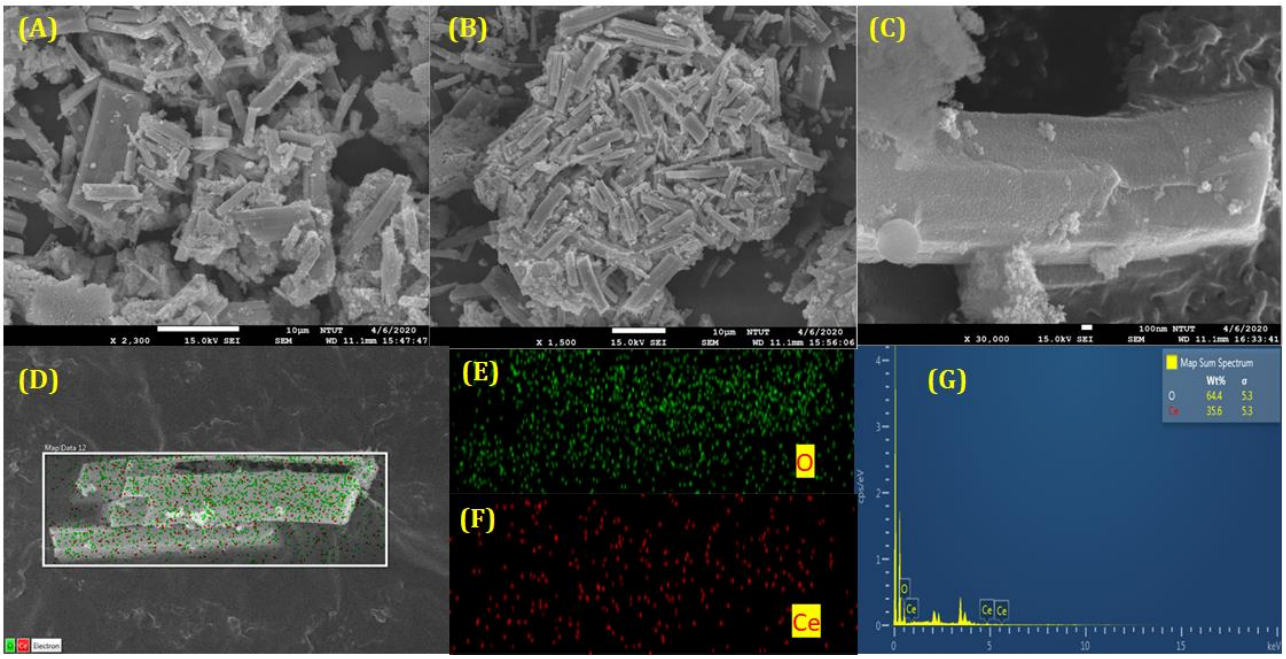

Figure 2. (A-C) FE-SEM image of CeO_2 NRs, **(D)** Elemental composition of CeO_2 NRs, **(E)** O, **(F)** Ce, **(G)** The corresponding EDAX analysis of CeO_2 NRs

FE-SEM was used to characterize the morphology of as-synthesized cerium oxide nanorods. The obtained SEM images clearly showed the formation of rod-shaped cerium oxide nanoparticles, as shown in Figure 2 (A-C). Figure 2A and B shows that there are many even and regular-surfaced nanorods with good uniformity with even distribution. Especially, Figure 2C clearly shows the single nanorod observes at 100 nm magnification. Figures 2D, E, and F show the elemental distribution of as-prepared material and it's undoubtedly express only for Ce and O elements are present in the CeO_2 NRs. Figure 2G exhibits the elemental composition that the peaks for corresponding to cerium and oxygen and it was confirmed the Ce and O elements present in as-synthesized CeO_2 NRs.

3.2 Electrocatalytic activity of CeO_2 NRs toward ISPN oxidation

The electrochemical technique namely EIS was used to investigate the surface properties and electron transfer kinetics of CeO_2 NRs/GCE. Figure 3A shows the EIS curve for CeO_2 NRs/GCE (blue), bare GCE (red) solution containing in 5.0 mM $K_3[Fe(CN)_6]^{3-/4-}$ and 0.1 M KCl at a frequency range 0.01 to 100 kHz. From Figure 2C, to observe the charge transfer resistance (Rct) of CeO_2 NRs/GCE is much higher than the bare GCE. This result suggesting the CeO_2 NRs modified electrode has rapid electron transferability.

Figure 3B shows the CV response of unmodified GCE (a), CeO_2 NRs fabricated GCE (b). The experiment was recorded in a solution containing 100 µM ISPN in an aqueous solution of pH 7.0 (PBS, 0.05 M) of a potential window from 0 to 0.6 V at a sweep rate of 50 mV/s. Figure 3B, (peak a) is the bare glassy carbon electrode towards 100 µM of ISPN and it shows a weak anodic peak current. However, the cerium oxide NRs modified glassy carbon electrode observed well oxidation peak current

with lower oxidation potential is shown in Figure 3A (peak b). This result indicates the CeO_2 NRs have superior electron transfer properties and enhance the electrocatalytic activity of ISPN sensing. CV response of CeO_2 NRs modified GCE in 0 – 250 μM of ISPN in pH 7.0 PBS at 50 mV/s, as shown in Figure 3C. The anodic peak current of ISPN was increased linearly with increasing the ISPN concentration (0 – 250 μM). Figure 3D shows the corresponding linear plot against the obtained anodic peak current and ISPN concentration. The good linearity with the correlation coefficient is expressed as, I_{pa}=0.0312x+ 1.354 (R^2=0.998). This result indicates that the CeO_2 is a good electrochemical catalyst for the ISPN oxidation.

3.3 Effect of potential scan rate

Further to investigate the sweep rate effect of ISPN by CV on CeO_2 NRs modified glassy carbon electrode at potential window 0 to 0.6 V in a solution containing 100 μM ISPN in pH 7.0 PBS. Figure 4C shows the anodic peak current (I_{pa}) of ISPN was increased upon increasing the sweep rate from 20 to 200 mV/s. Figure 4D illustrates the good linear plot that was observed from the anodic peak current of ISPN and the log of sweep rate with a correlation coefficient of R^2=0.996. However, the anodic peak potential is lightly shifted to the anodic side while rising the sweep rate, demonstrating the kinetic limitation of the electrochemical reaction. This result proposed that the electrochemical oxidation of ISPN on CeO_2 NRs fabricated glassy carbon electrode is controlled by the diffusion process [10].

3.4 Effect of pH electrolyte

The electrochemical oxidation of ISPN involves the participation of electron and proton. The supporting electrolyte generally deep effect on electrochemical behavior. Meanwhile, the effect of pH on CeO_2 NRs fabricated electrode towards the ISPN oxidation in the pH range of (5.0 – 9.0) with a sweep rate of 50 mV/s, the result is shown in Figure 4A. As can be seen from Figure 4A, the anodic peak potential with the current increased when the pH increased from 5.0 – 7.0, and then anodic peak potential (E_{pa}) with anodic peak current (I_{pa}) conversely decreased when the pH is increased from 7.0 – 9.0. This result shows the maximum value of the electrocatalytic current has observed at a pH medium of 7.0 [22]. So, neutral pH 7.0 was used as a supporting electrolyte throughout the experiment. As well as, Figure 4B reveals the good linear relationship with a correlation coefficient of R^2=0.0997. Such behavior proposes the number of transfer electrons and protons are equal in ISPN oxidation. Scheme 1 illustrates the schematic representation of this work.

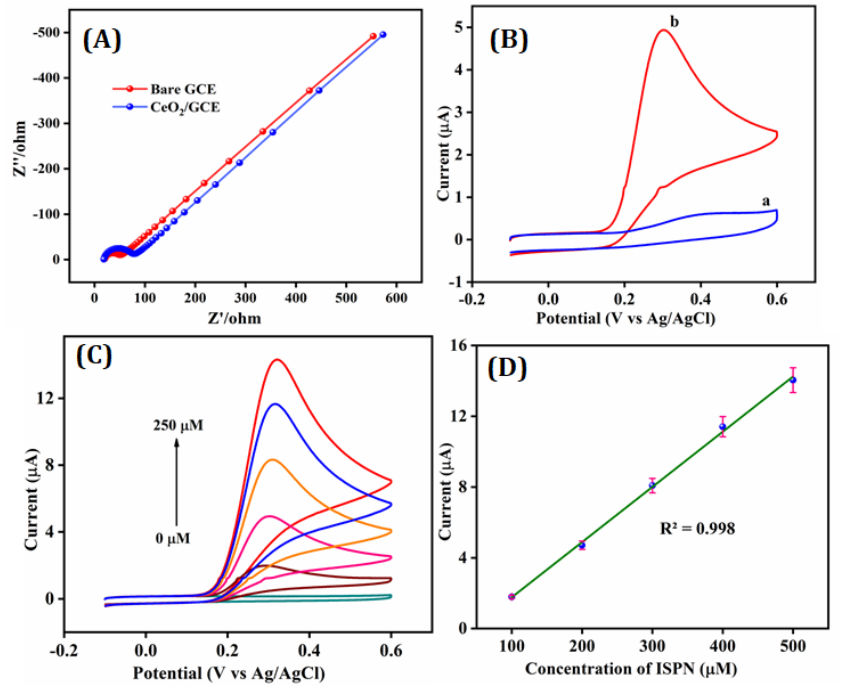

Figure 3. (A) EIS curve for CeO_2/GCE (blue), unmodified GCE (red) in 0.1 M KCl, 5.0 mM $K_3[Fe(CN)_6]^{3-/4-}$, **(B)** CV profile for the CeO_2 NRs modified electrode (b), bare GCE (a), **(C)** CV response for CeO_2 NRs/GCE at concentration range (0-250 µM) **(D)** The corresponding linear plot of anodic peak current vs. ISPN concentration.

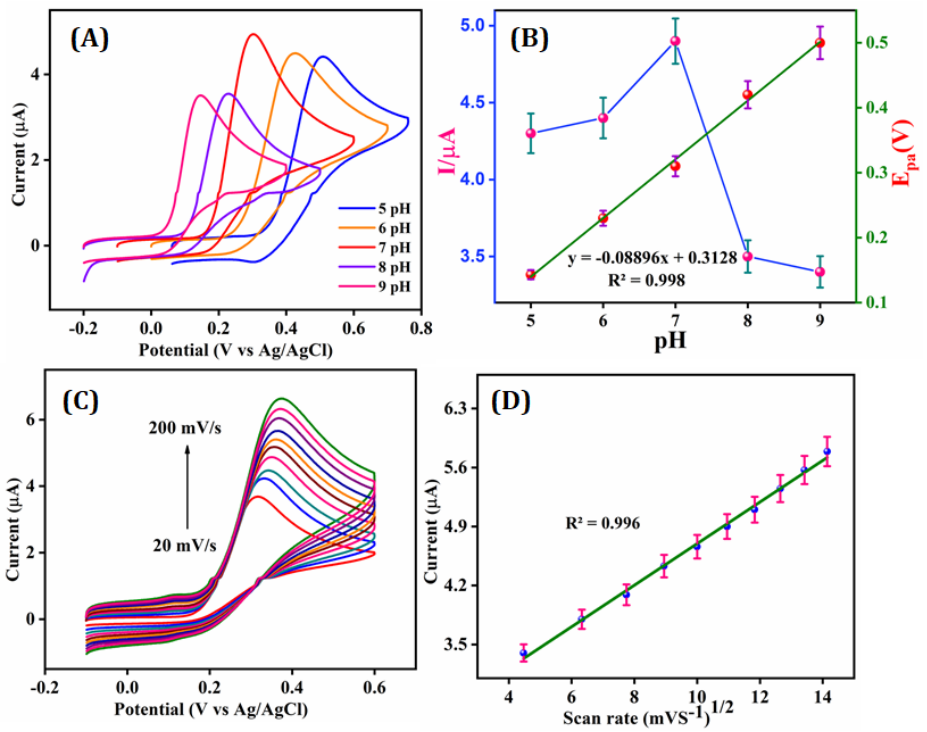

Figure 4. (A) CV response of different pH (5.0 – 9.0) in the presence of 100 µM ISPN in 50 mV/s, **(B)** The plot between different pH vs peak potential (green line), The plot between different pH vs anodic peak potential (blue line), **(C)** CV response of CeO_2 NRs in pH 7 at different scan rate range from 20 to 200 mV/s **(D)** The linear plot between anodic peak current versus log of scan rate

3.5 Determination of ISPN on CeO_2 NRs/GCE

In this study, the more conscious DPV technique was applied to obtain the limit of detection (LOD) and dynamic linear range of ISPN. Figure 5A displays the DPV curve for the oxidation peak current of ISPN carried out by modifying GCE with CeO_2 NRs in the solution of pH 7.0. From Figure 5A the oxidation peak current of ISPN increases while increasing the concentration of ISPN from 0.04 to 1219 µM. The corresponding linear range of well-separated electrooxidation peak current versus ISPN concentration shown in Figure 5B. The good linearity with the correlation coefficient equation is expressed as; I(µA)=0.0143x–0.0007, (R^2=0.993). From the corresponding linear plot, the detection limit is calculated as 18 nM. The kinetic parameters such as the limit of detection and dynamic linearity for the proposed CeO_2 NRs modifying GC electrode were compared with earlier reported other electrode materials, shown in Table 1.

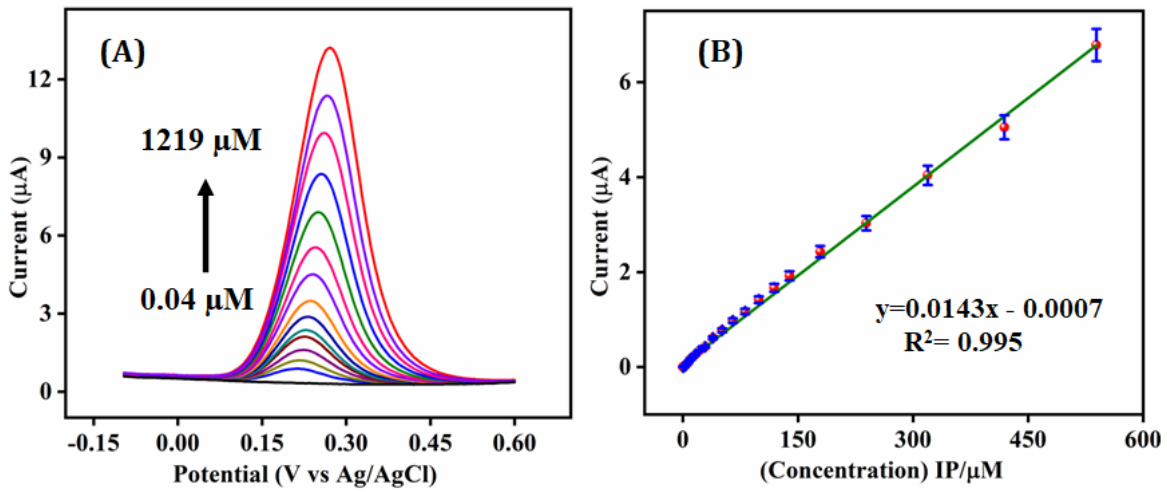

Figure 5. (A) DPV signals of CeO_2 NRs/GCE at different concentration of ISPN (0.04 –1219 µM) in pH 7.0 (PBS, 0.05 M), **(B)** the good linear plot of oxidation peak current versus ISPN concentration (0.04 – 539 µM)

Table 1. Comparison of kinetic parameters such as linear range, limit of detection for the proposed ISPN sensor based on with previously reported sensor

Electrode	Method	Linear range (µM)	Limit of Detection (nM)	Ref
CuHCF[a]/CPE[b]	CV	196–1070	800	2
ZnONP-IL/CPE[b]	SVW	–	90	6
MC-CNPE[c]	DPV	0.7–600	35	22
Poly(1-methylpyrrole)-DNA	CV	2.0–60.0	160	23
FMA/CNTPE[d]	DPV	0.5–50.0	200	24
GCE/AuNPs/DPB[e]	DPV	0.1–900	82	25

CPMBD[f]/TiO_2NPs/CPE	DPV	-	470	26
Lac[g]-SiSG/MWCNT[h]/GCE[i]	CA	-	180	27
DDTA[j]/CNPs/CPE	DPV	-	75	28
CeO_2 NRs/GCE	DPV	0.04 –539	18	This work

[a]Copper(II)hexacyano ferrate (III), [b]carbon paste, [c]molybdenum (VI) complex-carbon nanotube paste, [d]ferrocenemonocarboxylic acid modified carbon nanotubes paste electrode, [e]2-(2,3-dihydroxy phenyl) benzothiazole, [f](E)-2-((2-chlorophenylimino) methyl) benzene-1,4-diol, [g]laccase, [h]multiwalled carbon nanotubes, [i]glassy carbon electrode, [j]7-(3,4-dihydroxyphenyl)-10,10-dimethyl-9,10,11,12-tetrahydrobenzo[c]acridin-9 (7H)-one

3.6 Interference, stability, and reproducibility

To determine the selectivity of the as-designed sensor was studied in the presence of various biologically active substances, some cations, and anions. Under the optimum experimental conditions, DPV was carried out in the presence of ISPN with 10-fold of glucose, fructose, acetaminophen, L-lysine, uric acid, glutamic acid, penicillamine, glycine, L-tyrosin, and piroxicam and also 100 fold excess of Na^+, K^+, Cl^-, Ca^{2+}, Pb^{2+} did not interfere the obtained DP voltammogram current response. This result reveals that the proposed ISPN sensor possesses good selectivity on CeO_2 NRs/GCE. The reproducibility of the fabricated ISPN sensor was carried out five different electrodes were fabricated by the same procedure and comparing the observed peak current towards the oxidation of ISPN. The obtained RSD of the CV peak current was about 3.4 %, and this result reveals that the CeO_2 NRs/GCE had appreciable reproducibility. The long-term stability was confirmed on the fabricated electrode. The CeO_2 NRs fabricated glassy carbon electrode was kept in our laboratory for 24 days at room temperature. Meantime, next 8, 16, and 24 days the respective peak current of the ISPN was received about 99.01 %, 98.16%, 96.48 %, and 94.23 % respectively, compared with newly fabricated electrode.

3.7 Determination of ISPN in Real sample

To inspect the practical applicability of CeO_2 NRs/GCE sensor to the detection of ISPN in human urine samples was examined by DPV. The found recovery results are listed in Table 2. The observed results indicate the determination of ISPN using the proposed electrode is more effective and can be successfully utilized for ISPN detection in real samples.

Table 2. Real-time determination of ISPN in human urine sample using CeO_2 NRs fabricated electrode

Sample	Added (µM)	Found (µM)	Recovery (%)
Urine	0	<LOD	-
	0.6	0.5	95.7
	1.3	1.2	98.27
	1.5	1.5	102.5

4. CONCLUSION

In the present work, the co-precipitation method was used for the preparation of electroactive cerium oxide nanorods, and it had performed as a good sensing platform for the determination of ISPN. The result of XRD, EDS, FT-IR confirmed the successful preparation of pure CeO_2. The suggested sensor exhibits a good linear response towards the determination of ISPN and LOD is 18 nM. Furthermore, the fabricated sensor also showed an acceptable selectivity, reproducibility, and stability towards the determination of ISPN. The analytical applicability of the fabricated electrode exhibits an exceptional real-time application with a human urine sample.

References

1. M. Sakr, R. Hanafi, M. Fouad, H. Al-Easa, and S. El-Moghazy, *Spectrochim. Acta, part A*, 208 **(**2019) 114.
2. V. G. Bonifcio, L. H. Marcolino Jr, M. F. Teixeira, and O. Fatibello-Filho, *Microchem. J. 78* (2004) 55.
3. A. A. Ensafi, and H. Karimi-Maleh, *Drug Test Anal. 3* (2011) 325.
4. M. Mazloum-Ardakani, S. H. Ahmadi, Z. S. Mahmoudabadi, and A. Khoshroo, *J. Braz. Chem. Soc*. 25 (2014) 1630.
5. N. Dhanalakshmi, T. Priya, S. Thennarasu, V. Karthikeyan, and N. Thinakaran, *J. Electroanal. Chem*. *848* (2019) 113283.
6. H. Karimi-Maleh, S. Rostami, V. K. Gupta, and M. Fouladgar, *J. Mol. Liq*. 201 (2015) 102.
7. S. Khezri, M. Bahram, and N. Samadi, *Spectrochim. Acta A*, 189 (2018) 522.
8. H. Beitollahi, and S. Nekooei, *Electroanalysis*, 28 (2016) 645.
9. G. J. Zhou, G. F. Zhang, and H. Y. Chen, *Anal. Chim. Acta*, 463 (2002) 257.
10. M. Mazloum-Ardakani, A. Naser-Sadrabadi, M. A. Sheikh-Mohseni, H. Naeimi, A. Benvidi, and A. Khoshroo, *J. Electroanal. Chem*. 705 (2013) 750.
11. M. Chen, X. Ma, and X. Li, *J. Solid State Electrochem*. 16 (2012) 3261.
12. X. Tong, T. Luo, X. Meng, H. Wu, J. Li, X. Liu, X. Ji, J. Wang, C. Chen, and Z. Zhan, *small*, 11 (2015) 5581.
13. A. Umar, R. Kumar, M. S. Akhtar, G. Kumar, and S. H. Kim, *J. Colloid Interface Sci*. 454 (2015) 61.
14. C. Zhang, F. Meng, L. Wang, M. Zhang, and Z. Ding, *Mater. Lett*. 130 (2014) 202.
15. L. Wang, F. Meng, K. Li, and F. Lu, *Appl. Surf. Sci*. 286 (2013) 269.
16. A. Sangili, M. Annalakshmi, S. M. Chen, T. W. Chen, S. Kumaravel, and M. Govindasamy, *Int. J. Electrochem. Sci*. 13 (2018) 6135.
17. G. Manibalan, G. Murugadoss, R. Thangamuthu, M. R. Kumar, R. M. Kumar, and R. Jayavel, *Inorg. Chem. Commun. 113* (2020) 107793.
18. S. A. Sayyed, N. I. Beedri, V. S. Kadam, and H. M. Pathan, *Bull. Mater. Sci*. 39 (2016) 1381.
19. J. Wang, Z. Li, S. Zhang, S. Yan, B. Cao, Z. Wang, and Y. Fu, *Sens. Actuators B,* 255 (2018) 862.
20. M. M. Ali, H. S. Mahdi, A. Parveen, and A. Azam, *AIP Conf. Proc*. 1953 (2018) 030044.
21. G. Jayakumar, A. A. Irudayaraj, and A. D. Raj, *Appl. Phys. A*, 125 (2019) 742.
22. H. Beitollahi, and I. Sheikhshoaie, *Electrochim. Acta*, 56 (2011) 10259.
23. A. Kutluay, and M. Aslanoglu, *Acta Chim. Slov*. 57 (2010) 157.
24. A. A. Ensafi, and H. Karimi-Maleh, *Int. J. Electrochem. Sci*. 5 (2010) 1484.
25. M. Mazloum-Ardakani, A. Dehghani-Firouzabadi, M. A. Sheikh-Mohseni, A. Benvidi, B. B. F. Mirjalili, and R. Zare, *Measurement*, 62 (2015) 88.
26. M. Mazloum-Ardakani, L. Hosseinzadeh, A. Khoshroo, H. Naeimi, and M. Moradian, *Electroanalysis,* 26 (2014) 275.

27. P. Gopal, T. M. Reddy, C. Nagaraju, and G. Narasimha, *RSC Adv*. 4 (2014) 57591.
28. M. Mazloum-Ardakani, N. Rajabzadeh, A. D. Firouzabadi, A. Benvidi, and M. Abdollahi-Alibeik, *Anal. Methods*, 6 (2014) 4462.